Some Challenges of QPE in Snow

Elena Saltikoff [1], Harri Hohti[1] and Philippe Lopez[2]
[(1)]*Finnish Meteorological Institute, P.O.Box 503, 00101 Helsinki Finland*
[(2)]*ECMWF, Shinfield Park, Reading, RG2 9AX, United Kingdom*

(Dated: 17 July 2014)

Elena Saltikoff

1 Introduction

From a hydrological point of view, radar is a device measuring rainfall. So far, less attention has been paid to snowfall. However, melting snow can cause flooding in some areas and is a source to hydropower in other regions. To estimate the amount of melting snow, accurate and especially unbiased measurements of snowfall amount are needed.

Typically, radar measurements of reflectivity (Z) are converted to rainfall intensity (R) using empirical equations of the form $Z = aR^b$, where parameters a and b are usually determined from a large set of measurements. A widely used combination of these two parameters is a = 200 and b = 1.6 (Marshall and Palmer, 1948; Marshall et al, 1955). Battan (1973) published a review of sixty-nine other pairs of a and b values valid for different climates and precipitation types.

For snowfall, fewer equations have been published, and the range of parameters a and b is expected to be even larger than for rainfall.

Finnish Meteorological Institute (FMI) uses different equations for rain and snow (see below) to convert radar reflectivity, Z, into precipitation intensity (R or S, in mm/h). For rain, equation (1.1) from Dölling et al. (1998) is used. For snow, equation (1.2) based on Sekhon and Srivastava (1970) was used until 2004. However, the end users reported an underestimation of snowfall and equation (1.3) was therefore implemented. It was recently noticed that Zhang et al. (2014) had used a very similar equation for NEXRAD (1.4). Marshall-Palmer equation (1.5) is also used as a default in many applications, including OPERA. The Z-R and Z-S formulae are given as

$$Z = 316\, R^{1.5} \qquad (1.1)$$

$$Z_e = 398\, S^{2.21}. \qquad (1.2)$$

$$Z_e = 100\, S^{2}. \qquad (1.3)$$

$$Z_e = 75\, S^{2}. \qquad (1.4)$$

$$Z = 200\, R^{1.6} \qquad (1.5)$$

where R denotes the rainfall intensity and S the snowfall intensity. Z_e is the equivalent radar reflectivity factor, which differs from the cloud physical definition of Z, because the dielectric constant used in the radar processing algorithm applies to water, not snow.

Figure 1 displays a comparison of the above equations for snow against the Marshall-Palmer equation (1.5), which is used as a reference in many applications. For low reflectivities, all the dedicated snow equations give stronger intensities than the Marshall-Palmer equation. For high reflectivities, the Sekhon-Srivastava equation (1.2) gives significantly smaller intensities. Note that reflectivities higher than 40 dBZ are extremely rare in snowfall.

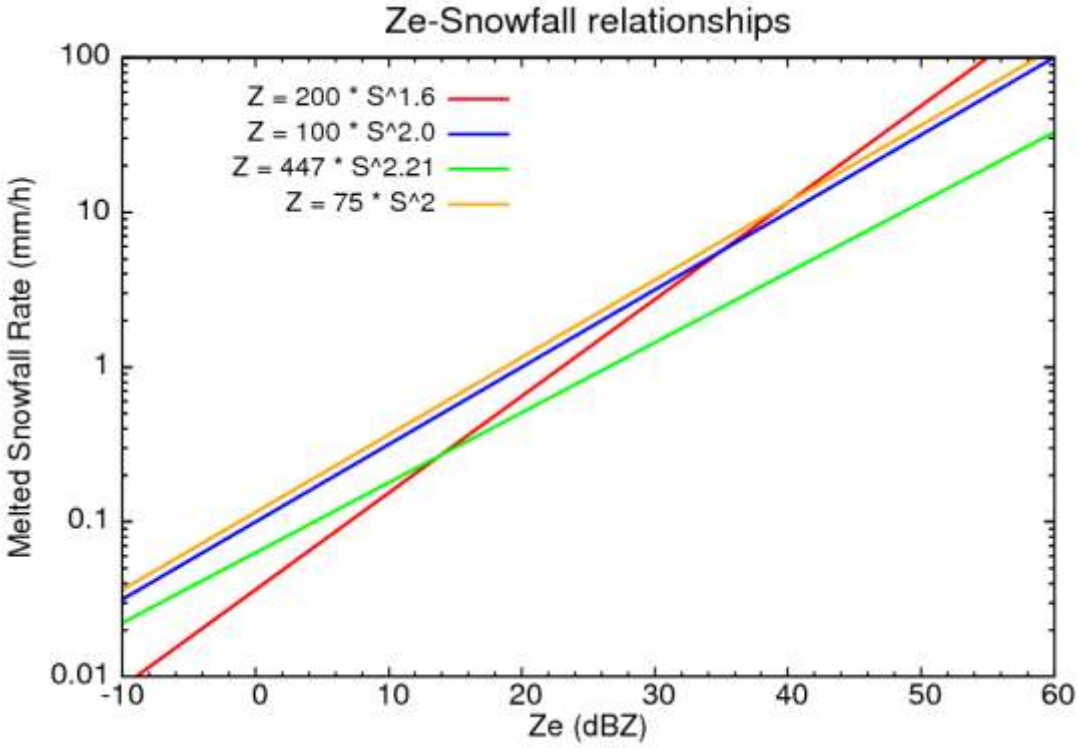

Fig.1. Comparison of different reflectivity-snowfall equations, Marshall Palmer equation (1.5) in red,. Sekhon and Srivastava (1.2) in green, 1.3 FMI operational snow (1.3) in blue, and NCEP/NEXRAD equation (1.4) in orange.

After FMI replaced the Sekhon-Shrivastava equation with equation (1.3), the end users were relatively happy. In Finland, the most important user for QPE in snow is the road maintenance sector (who are actually not so much interested in the water equivalent, but rather in the snow depth increase, but that is another issue). Data used in the present study were collected during the first winter when this equation was used operationally, but never published, mainly because we were aware that there is no "ground truth". Now that the use of that equation is spreading, it is time to review its performance again.

2 Known error sources

2.1 Radar error sources

The uncertainty factors affecting radar reflectivity are the electronic mis-calibration, beam blocking, and attenuation due to both precipitation (Battan, 1973) and wet radome (Germann, 1999). Vertical profile of reflectivity (VPR) has been mentioned as the greatest source of uncertainty in radar measurements in high latitudes, which leads to a range-dependent error (Zawadski, 1984). At large distances, the radar probes the upper parts of the cloud, where reflectivity is weaker. However, statistical correction methods have been developed and implemented in many countries, which also compensate for overestimation in the melting layer, when appropriate (e.g. Koistinen et al., 2003). As the effect is largest at long distances from radar, dense radar networks do not suffer from this phenomenon.

The overhanging precipitation issue refers to the case when precipitation is correctly measured aloft but evaporates before reaching the ground. This is most typical in association with warm fronts. Due to the three-dimensional structure of the frontal precipitation band, correction using vertical profile of reflectivity is difficult or impossible. Attempts to identify and eliminate the overhanging precipitation by using the NWP data have been made (Pohjola and Koistinen, 2004) but the results were not satisfactory mainly due to prediction errors related to the timing of the precipitation bands in the model.

Total beam overshooting occurs when the precipitation top does not extend to the height of the lowest radar measurement. This is typically associated with drizzle and snowfall, especially to snowfall in a cold climate. There is no obvious solution to this problem, apart from increasing radar network density. In Figure 2, one can identify radar-centered "roses" almost everywhere in cold regions, but the error only becomes significant at the edges of the image or in areas with low radar density (e.g. Eastern Finland, Ireland). These roses arise from VPR and from partial or total beam overshooting.

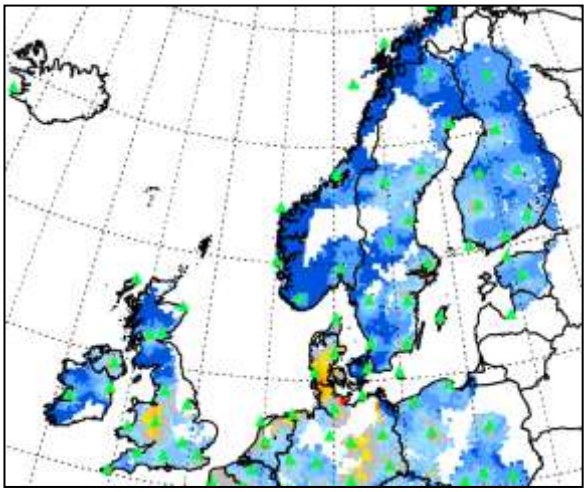

Fig.2. Difference between QPE by OPERA composite and ECMWF model fields in December 2013. The darker blue shades reflect larger underestimation by radars.

The concept of using one equation to convert radar reflectivities into precipitation intensities relies on the assumption that the particle size distribution is constant. Every day experience shows this is not the case for snowfall; indeed, Bentley (1931) had already claimed that there are no two similar snowflakes. More recently, Huang et al. (2014) used a 2D-video disdrometer to derive Z_e-S relations in four cases. Different snow types lead to different optimal Z-S relations. Operationally, the challenge lies in the determination of snow type. Unfortunately, optical disdrometers remain research instruments, which cannot be used operationally. Even if such observations were available locally, their representativity remains limited in space and time. Tollman et al (2008) compared particle density to manual observations of particle type during a warm front overpass (Fig 3), and noticed a great variability in both.

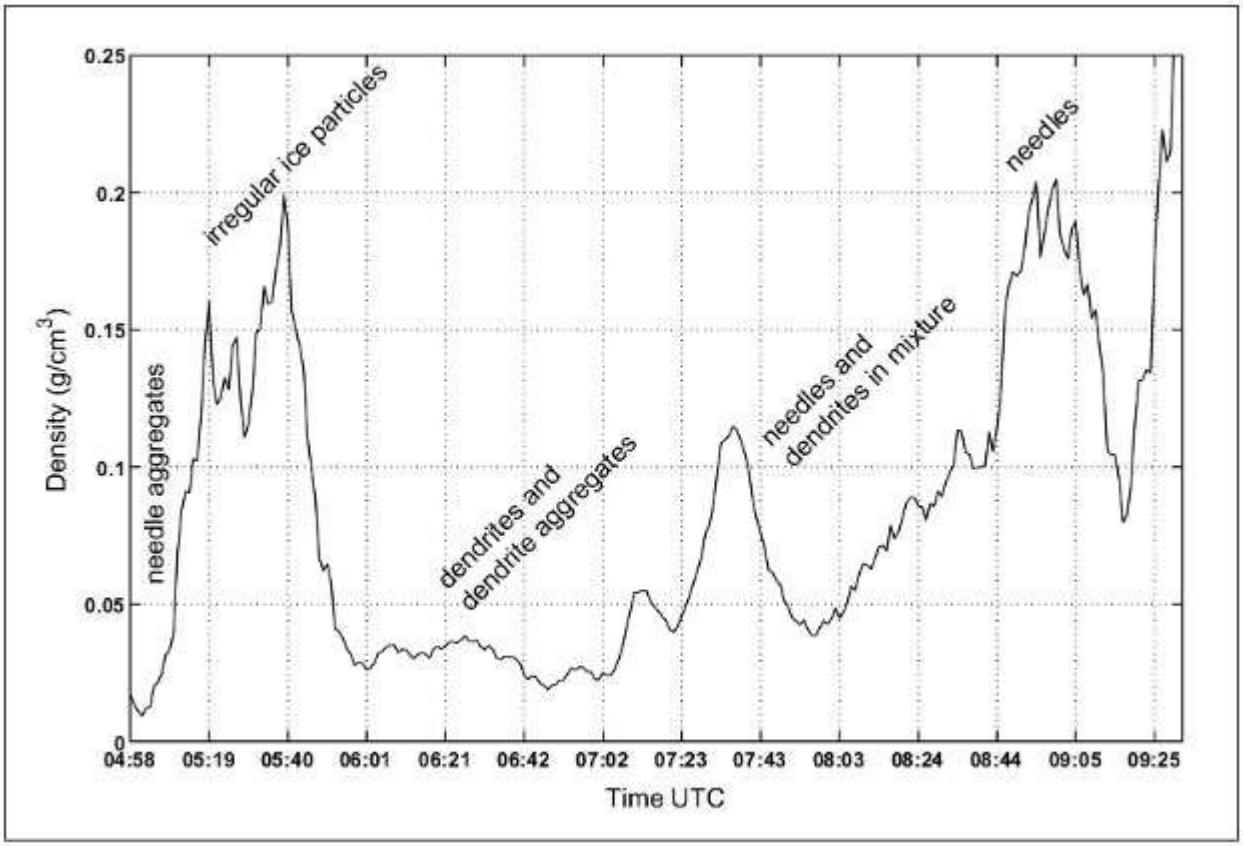

Fig.3. Density of snowfall and manual observation of particle type during one warm front overpass. From Tollmann et al, 2008.

2.2 Gauge error sources

The rainfall measured with manual gauges is almost always smaller than the actual rainfall. Error sources include evaporation from the gauge, wetting of the gauge walls, airflow around the gauge collector, unsuitable location, splashing, instrument errors and human errors. Especially for snowfall, the aerodynamic error is the largest, and most difficult to eliminate. The aerodynamic error depends on air flow conditions around the gauge, gauge-top height above ground, wind speed and precipitation type. One should note that gauge height is not at all standardized worldwide.

In northern Europe, the errors related to undercatch of snow are considerable. For instance, 5.2% of precipitation in Germany occurs as snow and 13.2% as a mixture of rain and snow. Errors due to wind- induced undercatch are estimated to 12.3 ± 3.1 % on average during winter, and to 5.6 ± 1.7 % during summer. In a long-term average, the total error has been estimated as 16.7% (Richter, 1995, Paulat et al, 2008)

When data is used for hydrological purposes, it is usually corrected for wind-induced error. However this is usually not the case for real-time measurements sent through the GTS, which are typically used in numerical weather prediction (NWP) applications (e.g. for nowcasting, model validation or data assimilation).

WMO has organized solid precipitation measurement intercomparison campaigns to estimate the errors for different gauge types. In cold temperatures (when snowflakes are light and fluffy) and strong wind the corrections factors for Tretjakov gauge can reach up to 3, which means that gauges may sometimes only collect around 30% of the actual snow (see Fig. 4 and 5, taken from Goodison et al, 1998)

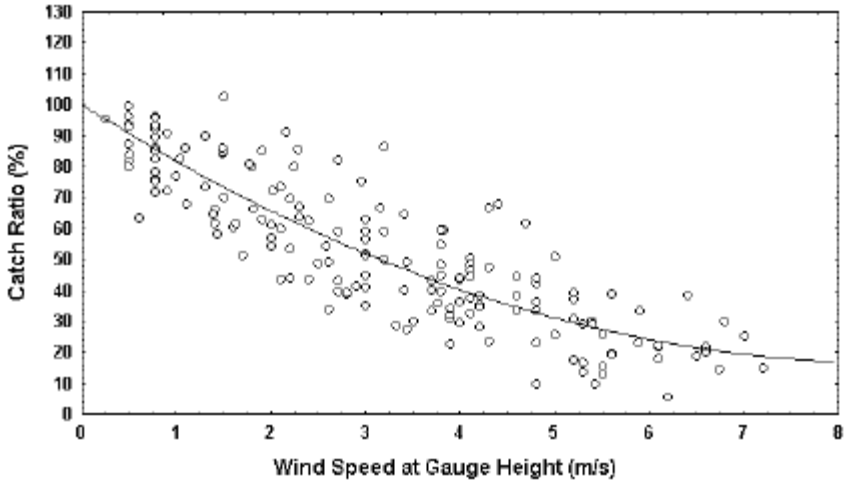

Fig.4. Hellman gauge catch ratio of snow as a function of wind speed. From Goodison et al.1998

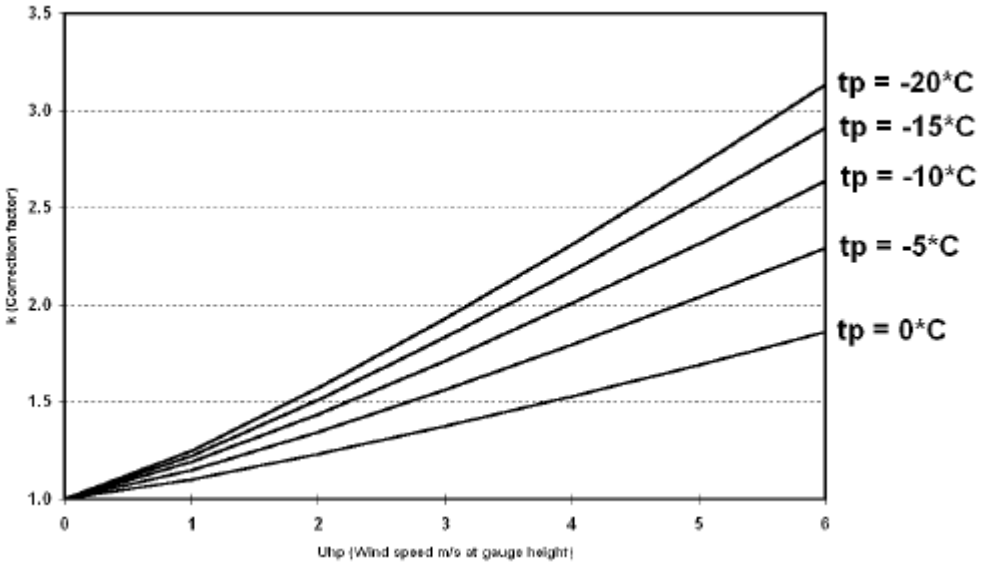

Fig.5. Relationship of correction factor (k, vertical axis) with wind (u, horizontal azis) and temperature for solid precipitation measured by the Tretyakov gauge. From Goodison et al 1998 and Braslavskiy et al.

The many types of automatic gauges currently in use are affected by different error sources. Heated tipping buckets are used in areas with short winters, but in serious conditions the evaporation loss can be significant. Automatic weighing gauges are another alternative in countries where the season with freezing temperatures is long. One serious operational problem with recording weighing gauges is that wet snow can stick to the gauge. Other problems include gauges catching drifting snow and wind-induced oscillation of the weighing mechanism (wind pumping) (Goodison et al, 1998)

Optical instruments, mainly developed as present weather sensors, can also be used for quantitative precipitation estimates. Wong (2012) has compared weighing gauges and optical instruments in Canada. In his study, one of the two optical instruments showed an overcatch, the second one an undercatch. The overcatch got worse with increasing wind speed, which clearly indicates that the error structure for optical instruments is different from that of manual or weighing gauges.

2.3 Representativity differences

A gauge measures a small volume near the ground, a radar measures large volume aloft. Hence, when comparing radars and gauges, an additional challenge arises from the different sampling sizes of these instruments.

Radar measurement volume can be several kilometres wide and high (one degree beam is ca. 4 km wide at a 250 km range), while the measurement area of a gauge is typically 400 cm^2 (weighting gauges) or 100 cm^3 (optical instruments).

At longer distances radar measures snow at rather high altitude. After the snowflakes have been measured, they may drift significant distances with the wind before reaching ground level. This is more serious for snow than for rain, because snowflakes fall with smaller fallspeeds. Hence the error produced by wind drift can cause significant difference from nominally co-located gauge measurements (Mittermeier et al.2004)

3 Data and methodology

3.1 Radar versus individual gauges

In the first part of this study, radar data were compared to 24 hour snowfall from FMI gauge stations. The period of the study was Dec 2004 and Jan 2005 and consisted of 385 gauges with 20,599 observations of snow accumulation. Since many gauge stations do not report temperature and even fewer report precipitation type (which may change during a warm front overpass), we selected a cold period and assumed that all precipitation was falling as snow.

Radar data were collected every 5 minutes. For the first dataset (ZR), reflectivities on CAPPI level of 700 m were converted to intensities using equation (1.1) (the “rain equation”) and then aggregated into 24h sums. Missing data were compensated with previous and earlier measurements. For the second dataset (ZS), same procedure was repeated with equation 1.3 (“the snow equation”). For the third dataset (ZS+VPR), corrections for vertical profile of reflectivity was applied before using equation (1.3). Note that cases where both gauge measurement and radar data in ZS were below 0.1 mm in 24 hours were excluded.

3.2 Scandinavian radar, gauge and model datasets

In the second part of this work, OPERA precipitation composites over Scandinavia were compared to SYNOP gauge observations and ECMWF model first guess fields over the period Dec 2012-Feb 2013. The composites are available every 15 min and with a spatial resolution of 2 km (Huuskonen et al, 2014). These data were accumulated over 6-hour periods (ending at 00Z, 06Z, 12Z and 18Z) prior to statistical computations. Only pixels that were flagged as valid precipitation data (i.e. not flagged as ’no data’ or ’undetected’) were retained in the accumulations. In the OPERA rainfall product, standard Z-R relationship by Marshall and Palmer is always used. For this study, the snowfall intensities were recalculated using an inversion method: in pixels identified as snow, R in OPERA rain rate product was converted back to reflectivity using Marshall-Palmer equation, and then the reflectivity to snowfall intensity using equation 1.3.

The second precipitation dataset used in this study are 6-hourly accumulations from synoptic stations via GTS. Note that not all countries provide 6-hourly gauge measurements in the GTS..

The third precipitation dataset consists of short-range forecasts obtained from ECMWF’s operational forecasting system, which is described in Courtier et al. (1994). The forecasts used here were all initiated at 00Z, and 6, 12, 18 and 24-hour forecast ranges were retrieved to match the corresponding 6-hourly precipitation accumulation periods. Forecast data were produced at the operational horizontal spectral resolution of T1279 (i.e. roughly 16 km) and with 137 levels in the vertical. In the comparison of radar with model data, precipitation amounts at OPERA 2-km pixels were averaged over each ECMWF model grid box (≈16 km) to avoid spatial representativity issues. Even though model forecasts are likely to be usually less accurate than SYNOP observations, they are used here in order to assess the significance of the differences found between radars and gauges. They also have a better spatial coverage than 6-hourly gauge data, even though the spatial resolution is worse.

The area covered by our "Scandinavian dataset" also encompasses most of Finland and Estonia and it is limited by longitudes 6ºE and 30ºE and latitudes 55ºN and 72ºN. In Lopez (2014), this area was compared to nine other geographical subdomains. The Alpine region would also be of interest for snow studies, but this is not an option as long as radars from Italy, Austria and Switzerland are not included in the OPERA composites.

4 First results

4.1 Radar versus individual gauges

From the comparison of radar to single gauges, one can see that differences between gauge and radar measurements depend on precipitation intensity (Figure 6). The weaker the intensity is, the larger the difference in the positive direction, which points to either an overestimation by the radar or an underestimation by the gauge. This is most common for precipitation amounts below 2 mm day^{-1}. On the other hand, in moderate and high intensity cases, one can find cases where radar underestimates precipitation. This underestimation depends on the distance to the radar and can be partially compensated with adequate vertical profile correction, as illustrated in Fig.7.

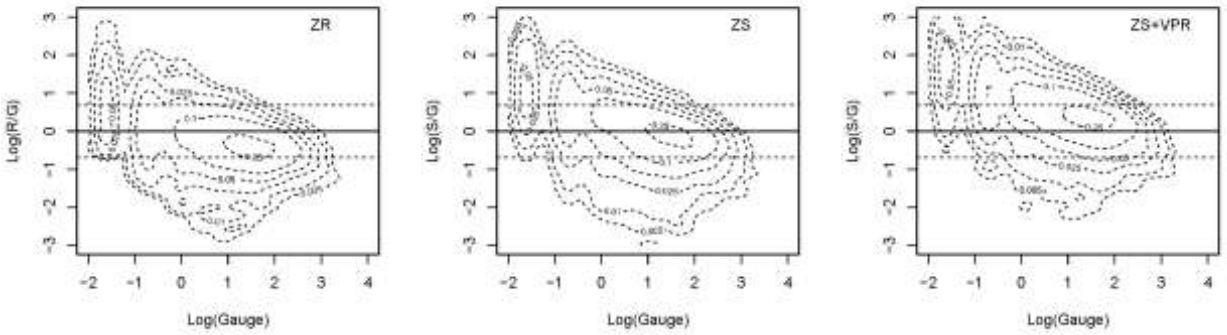

Fig.6. Logaritmic density plots of radar to gauge ratio versus gauge measurement using the ZR ratio for rain (left) snow (middle) and for snow, but with VPR correction before the ZS conversion (right). Solid line represents perfect match with gauges, dashed lines 50% and 200% of the latter.

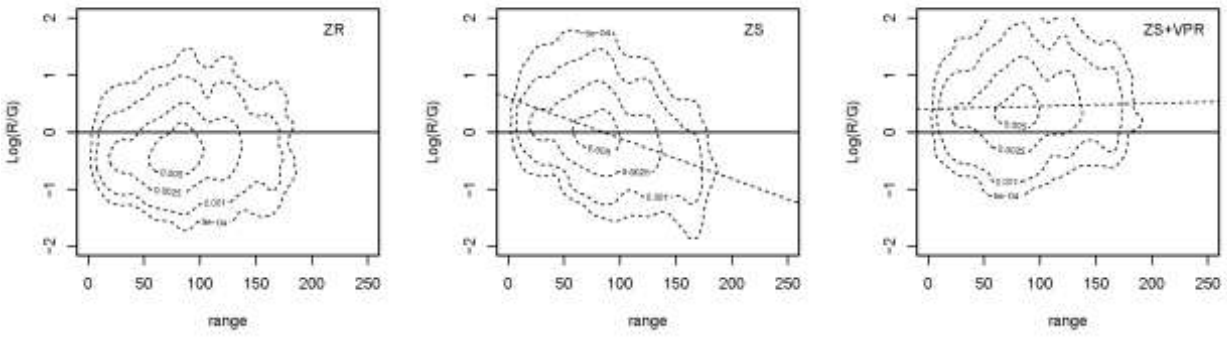

Fig.7. Radar-gauge ratios as function of range from radars (in km), using the ZR ratio for rain (left) and ZS for snow (middle) and for snow, but with VPR correction before the ZS conversion (right). Solid line represents perfect match with gauges, dashed lines are fits to the data.

As a result of implementing the FMI ZS equation and VPR correction, one obtain radar estimates that are higher than the gauge values, independent from the distance to the radar.

4.2 Scandinavian radar, gauge and model datasets

Time series of mean precipitation rate were calculated over all Scandinavia (using only the pixels where both data sources were available) and are displayed in Figs.8, 9, and 10. Figure 8 illustrates the well-known underestimation of snow when the Marshall-Palmer equation (1.1) is used. Using FMI's snow equation (1.3) brings the lines closer to both SYNOP and ECMWF model, as indicated by the mean values at the top of each panel. Implementing NCEP/NEXRAD's formula brings radar estimates even closer to SYNOP gauges and ECMWF model. However, this latter formula also tends to overestimate lighter snowfall amounts.

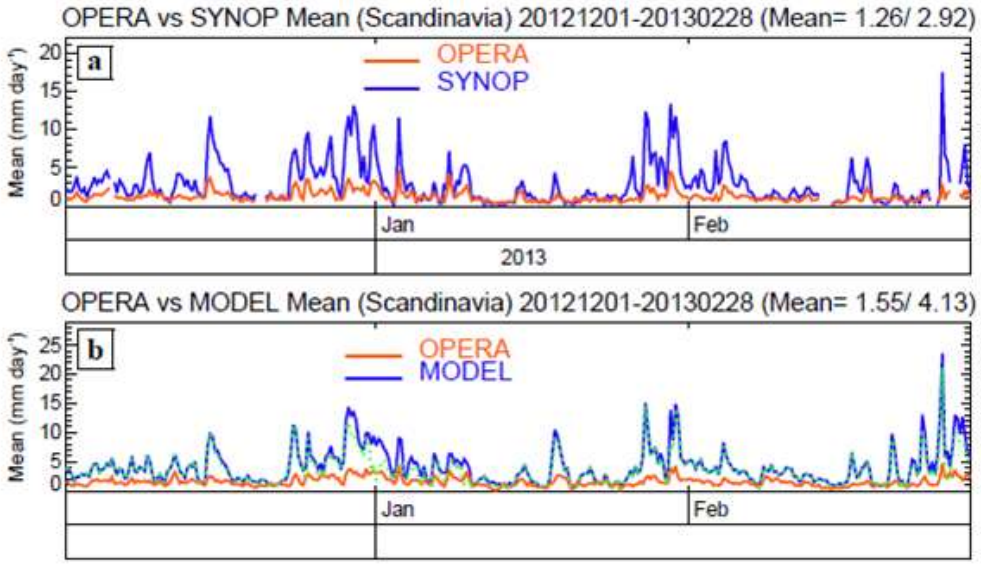

Fig.8. Time series of standard OPERA product versus (a) SYNOP and (b) ECMWF model 6-hourly precipitation accumulations averaged over Scandinavia between 1 December 2012 and 28 February 2013. Overall mean values are shown in the title in mm day for OPERA and the other dataset, respectively. The dotted green curve in panel (b) shows the amount of snowfall from the ECMWF model. Thus the vertical gap between the blue and green curves corresponds to the model's rainfall amount.

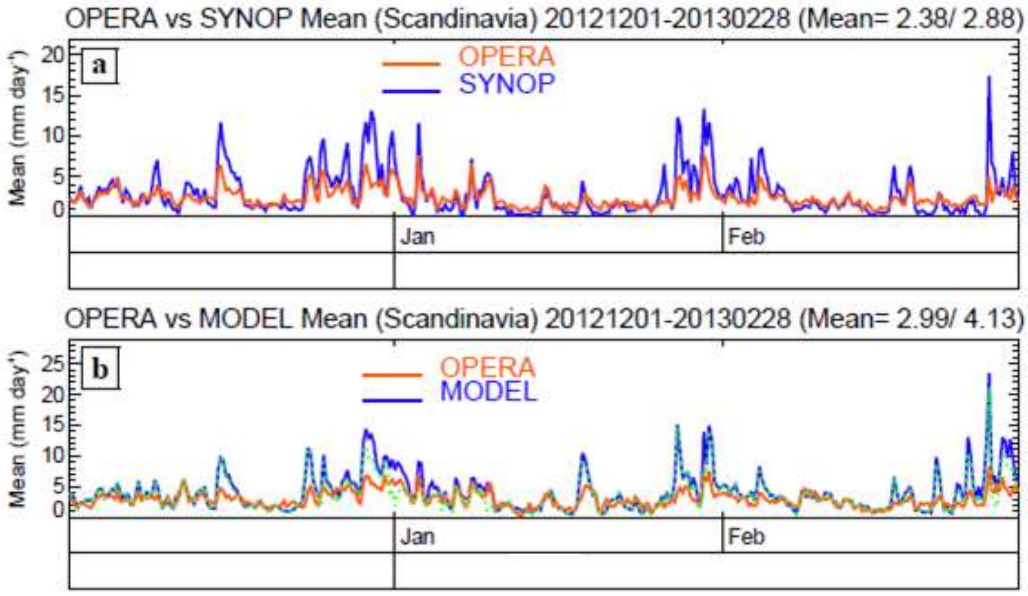

Fig.9. Same as Fig.8, but after recomputation of rainfall rates using equation (1.3).

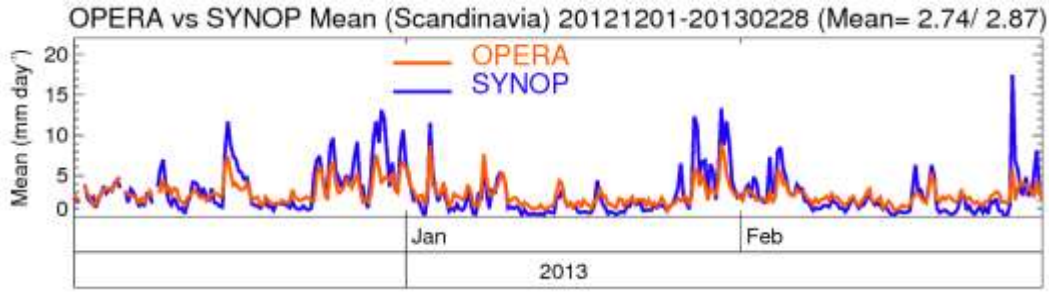

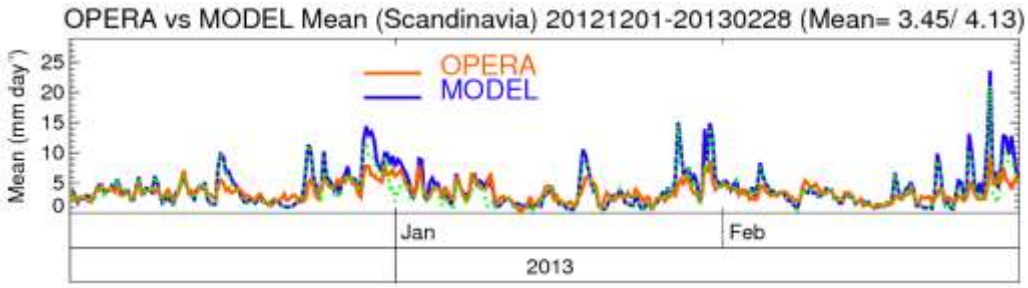

Fig.10. Same as Fig.8, but after recomputation of rainfall rates using equation (1.4).

It was also noticed, that if gauges were taken as ground truth, the false alarm rates of radar data for heavy snowfall (over 10 mm day^{-1}) in northern Europe would exhibit a maximum in late winter – February in Poland, March in Scandinavia. This is not seen if the model data is taken as ground truth. Potential explanations include gauge errors or the occurrence of the bright band in radar data – when comparing to the model, the 16 km calculation box would smooth the bright band maxima.

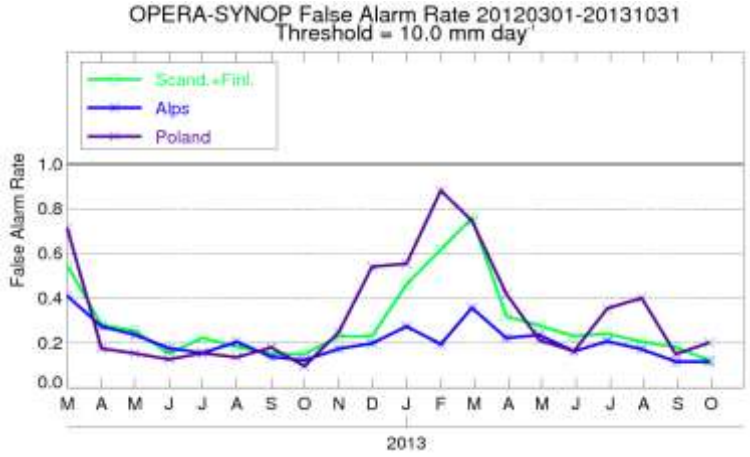

Fig.11. False alarm rate for heavy snowfall (over 10 mm day^{-1}) as function of time, over Scandinavia (green), Poland (purple) and the Alps (blue).

5 Conclusions and prospects

As a result of implementing the FMI ZS equation and VPR correction, we obtained radar precipitation estimates that are higher than the gauge values, regardless of the distance to the radar. We noted this in 2005, but we also knew that gauges are underestimating snowfall amounts. Hydrological services are part of another government office and at that time, wind correction of the gauge data was made on a monthly basis. However, they have recently been reprocessing historical data and shortly before the deadline of this abstract they sent us a dataset of daily corrected gauge data, which we sih to use in future work.

Changing the ZS equation does not alleviate all the issues related to the handling of snow in radar data processing. The OPERA team is currently working on the implementation of a correction procedure for the vertical profile of reflectivity in their European composites. Such procedure is already in operational use at FMI and many other national NMSes.

For NWP applications where model and radar observations need to be compared (e.g. model validation, data assimilation), an alternative approach is to compute simulated reflectivities from model output fields and compare these to observed radar reflectivities, rather than trying to retrieve precipitation from radar observations. This method has the potential to ensure a better consistency with the microphysical assumptions already made in the model physical parameterizations, provided, of course, that these are realistic enough. This is the method used in many limited area models.

Works by Tollmann (2008) and Goodison (1998) have shown that there exist a multitude of snow types, which can vary rapidly in time, in connection to but not fully explained by changes in temperature. Hence, the use of different ZS equations for different meteorological situations would be beneficial. Two challenges remain: first to derive those equations and second to determine when to apply each of them. Dual polarization radars are expected to help in this issue, but there is clearly still room for instrument and algorithm developments, both for in-situ and remote sensing instruments.

Acknowledgements

We would like to thank colleagues from Meteo-Swiss, Lorenzo Clementi and Marco Boscacci, for motivation to write this paper, and Minna Huuskonen at FMI and Kimmo Söderholm at SYKE for providing the corrected gauge data.

References

Battan, L. J., 1973: *Radar Observation of the Atmosphere*, University of Chicago Press, Chicago.

Germann, U 1999.: Radome attenuation – a serious limiting factor for quantitative radar measurements?, *Meteorol. Z.*, 8, 85–90, 1999

Goodison, B.E., Louie, P.Y.T. and Yang, D., 1998: *Final report of The WMO Solid Precipitation Measurement Intercomparison*. WMO.

Huang, G.-J. , Bringi, V.N., Moisseev, D., Petersen, W.A., Bliven, L. and Hudak, D., 2014: The Use of 2D-Video Disdrometer to Derive Mean Density-Size and Z_e-SR Relations: Four Snow Cases from the Light Precipitation Validation Experiment. Submitted to *Atmospheric Research*.

Huuskonen, A, and Holleman I and Saltikoff E, 2014 The Operational Weather Radar Network in Europe *Bull. Am. Met. Soc* ; doi: http://dx.doi.org/10.1175/BAMS-D-12-00216.1

Koistinen, J., Michelson, D. B., Hohti, H., and Peura, M. 2003: Operational Measurement of Precipitation in Cold Climates, in: Weather Radar Principles and Advanced Applications, edited by: Meischner, P., Springer, Germany, 337 pp.

Lopez, P., 2014: Comparison of ODYSSEY precipitation composites to SYNOP rain gauges and ECMWF. *ECMWF Technical Memorandum 717*. Available from ECMWF, Reading, United Kingdom.

Marshall, J. S. and Palmer, W. M.: 1948: The Distribution of raindrops with size, *J. Meteorol.*, 5, 165–166, 1948.

Marshall, J.S., Hitschfeld, W. and Gunn, K.L.S., 1955. Advances in radar weather. *Adv. Geophys* 1, 2 , 1–56.

Mittermaier, P.M., Hogan, J.R. and Illingworth, J.A., 2004: Using mesoscale model winds for correcting wind-drift errors in radar estimates of surface rainfall. *Quarterly Journal of the Royal Met. Soc*., 130, 2105-2123.

Paulat M, Frei C, Hagen M, 2008, A gridded dataset of hourly precipitation in Germany: Its construction, climatology and application. *Met. Zeitschrift* Vol. 17, No. 6, 719-732.

Pohjola H. and J. Koistinen 2004: Identification and elimination of overhanging precipitation Proceedings of ERAD (2004): 91–93 Copernicus GmbH. Available online at http://www.copernicus.org/erad/2004/online/ERAD04_P_91.pdf link accessed 17.7.2014

Richter, D., 1995: Ergebnisse methodischer Untersuchungen zur Korrektur des systematischen Mess-fehlers des Hellmann-Niederschlagsmessers. – *Berichte des Deutschen Wetterdienstes* 194, 93 pp (referred in English in Paulat et al, 2008, A gridded dataset of hourly precipitation in Germany: Its construction, climatology and application. *Met. Z* Vol. 17, No. 6, 719-732.

Saltikoff, E., Huuskonen, A., Hohti, H., Koistinen, J. and Järvinen, H., 2010: Quality assurance in the FMI Doppler Weather Radar Network. *Boreal Env. Res.* 15: 579–594.

Sekhon, R. and Srivastava, R., 1970: Snow Size Spectra and Radar Reflectivity. *J. Atmos. Sci.*, 27, 299–307.

Tollman, N., Göke, S., Leskinen, M. and Siivola, E., 2008: Characterizing rimed versus aggregated snow when analyzing the shape of hydrometeor size distributions. *ERAD 2008*, (CD–ROM).

Wong, K., 2012: Performance of Several Present Weather Sensors as Precipitation Gauges, in: *WMO TECO*, 16–18 October 2012, Brussels, Belgium, 25 pp.

Zawadzki, I. 1984: Factors affecting the precision of radar measurement of rain, in: 22nd Conference on radar meteorology, 10–13 September 1984, Zurich, Switzerland, 251–254.

Zhang, J. et al., 2014: Initial operating capabilities of quantitative precipitation estimation in the multi-radar multi-sensor system. 28th Conf. on Hydrology, Amer. Meteor. Soc. 2-6 Feb. 2014, Atlanta, GA. Paper 5.3. Available online at https://ams.confex.com/data/manuscript/ams/94Annual/Paper_240487_manuscript_1686_0.pdf. Link accessed 17.7.2014